Numerical simulation for symmetric diffraction patterns of 8-hydroxyquinolin-1-ium 4-aminobenzenesulfonate

A. Ghanem[1], M. D. Zidan[2]*, M. S. EL-Daher[1], and A. Allahham[2]

1. Higher Institute for Laser Research and Applications, Damascus University, Syria

2. Department of Physics, AEC, P. O. Box 6091, Damascus, Syria

©Tianjin University of Technology 2022

We reported the formation of diffraction ring patterns induced by transmitted Gaussian laser beam through 8-hydroxyquinolin-1-ium 4-aminobenzenesulfonate (8HQABS) solution as absorbing medium. Theoretical model depending on the Fresnel-Kirchhoff diffraction (FKD) theory was used to generate diffraction rings with respect to the sample position. Analysis of the generated diffraction rings shows a reasonable agreement between the features of the experimental and numerical diffraction rings. Our results are considered to be useful to understand the way of propagation and interaction of laser beam with liquid absorbing medium.

When the Gaussian laser beam passes nonlinear optical (NLO) materials, a diffraction ring pattern tends to appear in far field (on white screen)[1-4]. The formation of the diffraction ring pattern in far field was explained on the basis of the interference of many rays of the Gaussian light beam which came out parallel with the same wave vector and different phases after passing the NLO materials[1].

Performing the spatial self-phase modulation (SSPM) configuration will produce a diffraction ring pattern. When the phase distortion shift is larger than π, the SSPM mechanism leads to generation of self-diffraction rings around the propagation direction through the nonlinear absorbing medium[4]. The diffraction rings reveal some information about the NLO properties of the studied compounds. Also, the evolution time of the number of rings will be estimated. Since that phenomenon was observed for the first time by CALLEN et al[5], further works have been performed to study the NLO properties of newly prepared NLO materials[6-10].

In this work, diffraction ring patterns were generated in far field using a new salt of 8-hydroxyquinolin-1-ium 4-aminobenzenesulfonate (the new salt will be called as 8HQABS) with concentration of 10^{-3} M in ethanol using a continuous-wave laser with λ=532 nm. Then, a theoretical model depending on Fresnel-Kirchhoff diffraction (FKD) theory has been used to simulate the observed experimental diffraction rings in far field as a function of the sample position. Both, the numerical and the experimental diffraction rings were compared in order to clarify the applied FKD model. So, we can consider the novelty in our present work is the

comparative study between the theoretical model results and the observed experimental results at laser wavelength of λ=532 nm. Such study could be advantage of using the 8HQABS as working sample, which is considered to be a good candidate for use in photonic applications.

Considering a Gaussian beam TEM_{00} passes through nonlinear medium along z-direction, the input electric field at entrance plane of the sample can be expressed as[10,11]

$$E(r, z_0) = E(0, z_0)\exp(-\frac{r^2}{w_p^2})\exp(-\frac{\mathrm{i}k_0 n_0 r^2}{2R}), \qquad (1)$$

where $E(0, z_0)$ is the amplitude of the electric field, z_0 is the position coordinate of the medium entrance plane, $k_0 = \dfrac{2\pi}{\lambda}$ is the free space wavenumber, n_0 is the refractive index of the surrounded medium (air), $w_p = w_0\sqrt{1+\dfrac{z^2}{z_R^2}}$ is the beam waist at z, z_R is the diffraction length of the beam and $z_R = \dfrac{k w_0^2}{2}$, w_0 is the beam waist at the focus, and R is the curvature radius of the wave front at z and $R(z) = z(1+\dfrac{z_0^2}{z^2})$.

As a result of propagating Gaussian laser beam within the nonlinear medium, there would be absorption of the incident photons by the molecules inside the nonlinear medium, and energy exchanges between the molecules inside the sample. Therefore, the thermal effect of the

laser beam will lead to temperature dependent density variations in the sample solution, which causes the redistribution in refractive index $\Delta n(r, z)$ of the sample. Then, Δn is related to the absorbed light intensity I as

$$\Delta n(r, z)=n_2 I(r, z). \tag{2}$$

The relationship between the change in refractive index and the additional formula of the induced phase shift is given by[12]

$$\Delta \phi(r)=k_0 \int_{z_0}^{z_0+L} \Delta n(r, z)\, dz. \tag{3}$$

The complex amplitude of the electric field at the exit plane of the nonlinear materials will be[12]

$$E(r, z_0+L)=E(0, z_0)\exp\left(-\frac{r^2}{\omega_p^2}\right)\exp\left(-\frac{\alpha_0 L}{2}\right)\exp\left(-i\,\phi(r)\right), \tag{4}$$

where L, α_0 and $\phi(r)$ are the thickness of the sample, the linear absorption coefficient, and the total phase shift, respectively.

The total phase shift $\phi(r)$ is raised from two contributions. One is its own Gaussian phase shift described by the radius of wave front curvature R, and the other is the additional transverse phase shift $\Delta\phi(z_0)$ which originates after the beam propagation through the nonlinear medium. The following relation defines the two parts of total phase shift[10]:

$$\phi(r)=\frac{k_0 n_0 r^2}{2R}+\Delta\phi(r), \tag{5}$$

where

$$\phi(r)=k_0\int_{z_0}^{z_0+L}\Delta n(r, z)\, dz \approx \Delta\phi_0(z_0)\exp\left(-\frac{2r^2}{\omega_p^2}\right). \tag{6}$$

Then, Eq.(7) gives the total phase shift as

$$\phi(r)\approx k_0\frac{(n_0 r^2)}{2R}+\Delta\phi_0(z_0)\exp\left(-\frac{2r^2}{\omega_p^2}\right), \tag{7}$$

where $\Delta\phi_0(z_0)$ is the on-axis phase shift induced in the Gaussian beam when the sample is located at z_0.

By means of the FKD theory, the far field intensity distribution formula is given as[10]

$$I(\rho)\approx I_0\left|\int_0^\infty J_0(k_0, \theta)\exp\left[-\frac{2r^2}{\omega_p^2}-i\,\phi(r)\right]r\, dr\right|^2, \tag{8}$$

where $J_0(x)$ is the zero-order Bessel function of the first kind, θ is far-field diffraction angle and ρ is the radial coordinate in the far-field observation plane, which is given by $\rho=D\theta$, where D is the distance from the exit plane of the nonlinear medium to the far-field plane.

In the paraxial approximation, the two parameters I_0 and E_0 can be defined by Eqs.(9) and (10)[12,13] as

$$I_0=4\pi^2\left|\frac{E(0, z_0)\exp\left(-\frac{\alpha L}{2}\right)}{i\lambda D}\right|^2, \tag{9}$$

$$E_0=\frac{2}{w_0}\sqrt{\frac{P_0}{c\varepsilon_0 n_0 \pi}}, \tag{10}$$

where P_0 is defined as the output power of laser, c is the speed of light in vacuum, ε_0 is the permittivity of space, and n_0 is the refractive index of the surrounded air.

The 8HQABS salt has been characterized in our previous work[14]. The Z-scan experimental setup details were mentioned in our recent published work[15]. The closed-aperture Z-scan configuration has been demonstrated, in order to record typical normalized closed Z-scan plot of 8HQABS solution. The NLO effect of pure ethanol blank was neglected. Fig.1 shows the closed-aperture Z-scan of the 8HQABS solution, and the feature of the observed curve is peak-valley configuration. It can be deduced from the plotted curve that the phase shift is $\Delta\phi_0=8.79>2\pi$, so the dark and bright diffraction rings in far field will be observed[10,16,17]. Fig.1 shows the characterization of the laser spot shape after the propagating of Gaussian laser beam through the nonlinear medium in four specific regions according to the sample positions. When the sample was located far away from $z=0$, the NLO effect did not appear, only a laser spot. When the sample was moved close to the focal point ($z=0$), the detector recorded a maximum transmitted laser power, with the shape of the laser beam like a bright central spot. When the sample was moved a little away from the focal point, broaden diffraction rings could be observed as the transmitted laser power was dropped down. When the sample was moved far away from the focal point ($z=0$), no diffraction ring was observed, which was due to the absence the NLO effect. However, signs of curvature (R) changes accordingly are negative ($R<0$) and positive ($R>0$).
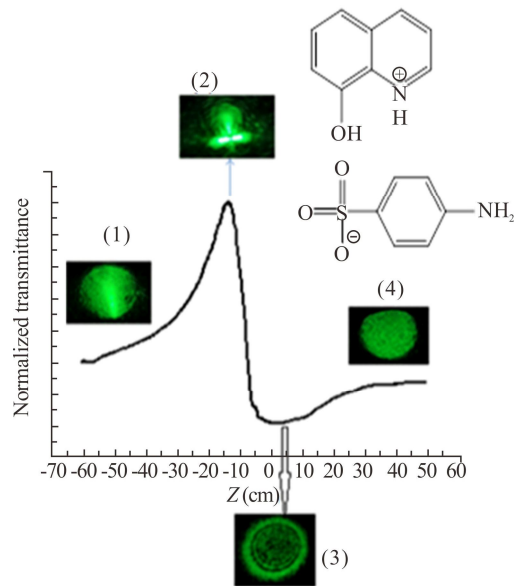

Fig.1 Closed aperture Z-scan result of 8HQABS solution

Fig.2 shows the experimental setup of the obtained

diffraction ring patterns. It consists of diode pumped solid state laser with Gaussian beam, a convex lens (*f*=10 cm) used to focus the laser beam inside the sample cell with thickness of 2 mm, and the screen located 140 cm away from the sample cell.
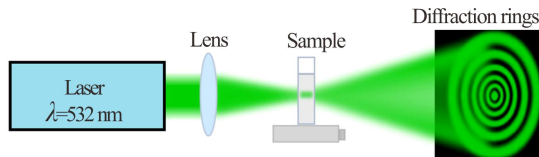

Fig.2 Experimental diagram of the SSPM technique

Fig.3(a) shows the numerical calculation of the intensity distribution of diffraction ring patterns at $z=-37$ mm using Eq.(8). Usually, the Gaussian laser beam causes changes in refractive index Δn in the nonlinear medium, which gives two cases as follows.

If $\Delta n<0$, the SSPM is induced and the medium will act as a negative lens making the beam divergent. When $\Delta n>0$, the medium acts as a positive lens and the beam will be focused. Our results have confirmed that the studied nonlinear medium can be considered as a self-defocusing material (peak-valley), which acts as a negative lens.

Simply, from Eq.(3) we can observe that the sign of $\Delta\phi(r)$ depends on Δn, therefore $\Delta\phi(r)<0$ in our sample. The experimental condition leads to two situations, namely, R and $\Delta\phi(r)$ have the same sign, and R and $\Delta\phi(r)$ are opposite in signs, which depend on sample positions from focal plane. Figs.3, 4 and 5 show the 2D normalized transmitted intensities of the beam when $R<0$ at three positions (before focal plane), the 3D theoretical curve, and the experimental diffractions rings.

We can see that when the sample is located before the focal plane ($R<0$), the taken snapshot of the laser beam shape in far field shows the bright sharp peak at the center. At the same time, our theoretical simulation using Eq.(8) has confirmed this point. Thin contiguous symmetric peaks around central bright sharp peak are presented as seen from Figs.3, 4 and 5. By locating the sample closer to the focal plane (Fig.5), the central bright peak still exsits, but the contiguous symmetric peaks become slightly broadened and have brighter intensity.

When the sample was translated away from the focal plane ($R>0$), we can observe from Figs.6, 7 and 8 that the central area is a dark spot, and there are remarkable thick bright rings surrounding the central dark spot. However, the bright diffraction rings look thicker gradually from the inner to the outer side, which means that the distribution of light energy will be in the outermost rings.

By analysis of our results, it can be concluded that the applied theoretical model performance is well consistent with the results of pervious reported works[12,13,16,18], as they performed similar theoretical and experimental works using different NLO media.
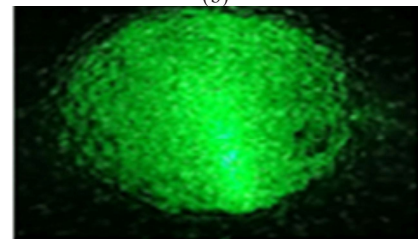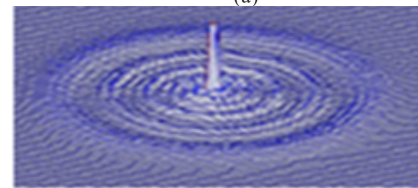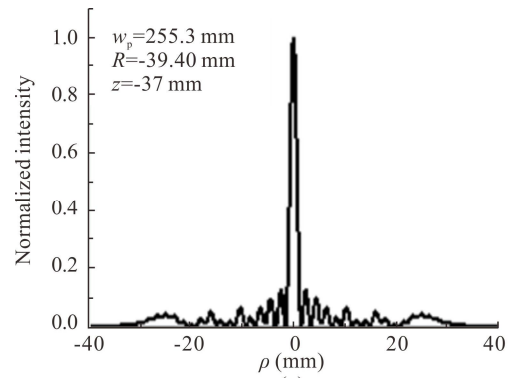

Fig.3 (a) Theoretical simulation result of the 2D intensity distribution at $z=-37$ mm by using Eq.(8); (b) 3D theoretical rings; (c) Experimental rings
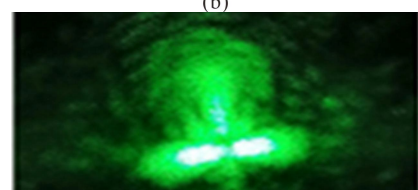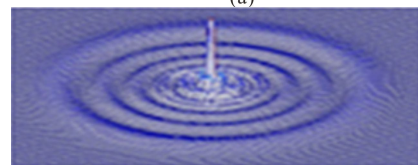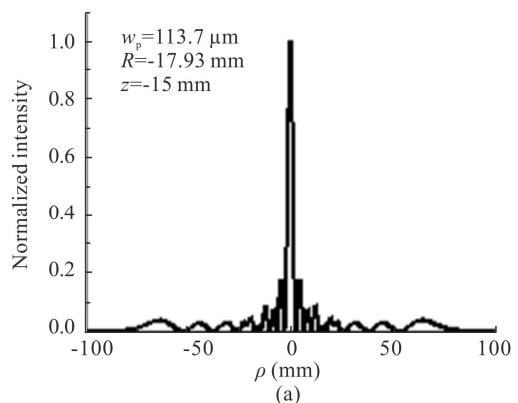
Fig.4 (a) Theoretical simulation result of the 2D intensity distribution at *z*=−15 mm by using Eq.(8); (b) 3D theoretical rings; (c) Experimental rings

w_p=70.1 mm
R=-11.59 mm
z=-8 mm

(a)

(b)

(c)
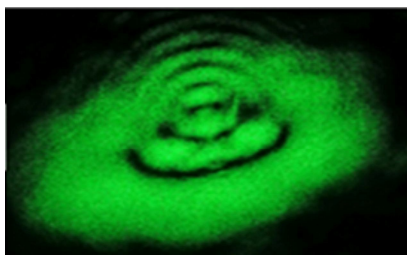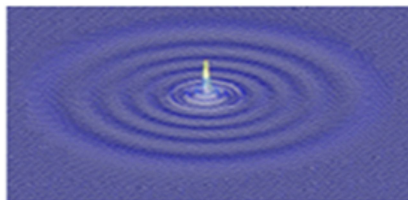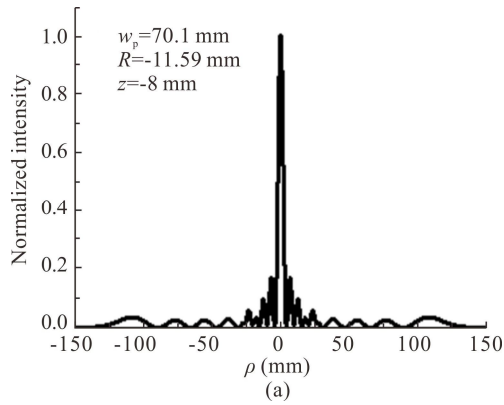
Fig.5 (a) Theoretical simulation result of the 2D intensity distribution at *z*=−8 mm by using Eq.(8); (b) 3D theoretical rings; (c) Experimental rings

w_p=58.2 μm
R=9.99 mm
z=+6 mm

(a)
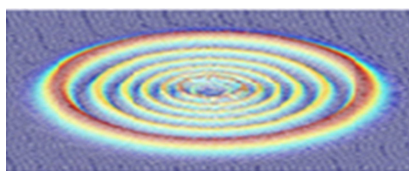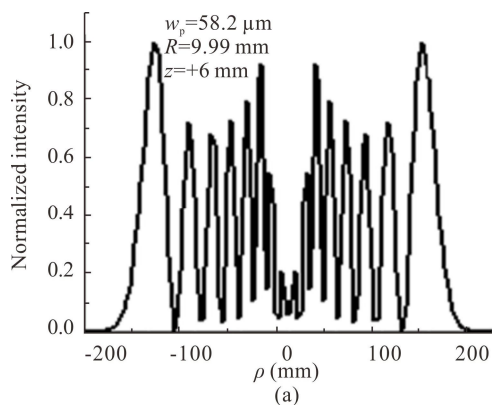
(b)
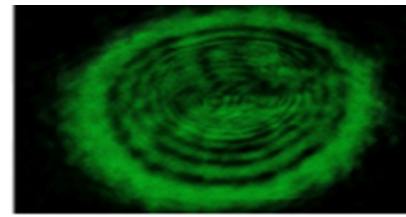
(c)

Fig.6 (a) Theoretical simulation result of the 2D intensity distribution at *z*=+6 mm by using Eq.(8); (b) 3D theoretical rings; (c) Experimental rings


w_p=94.8 mm
R=15.13 mm
z=+12 mm

(a)
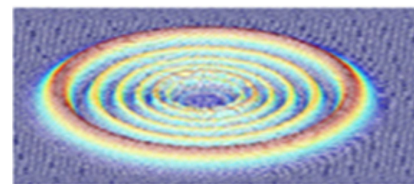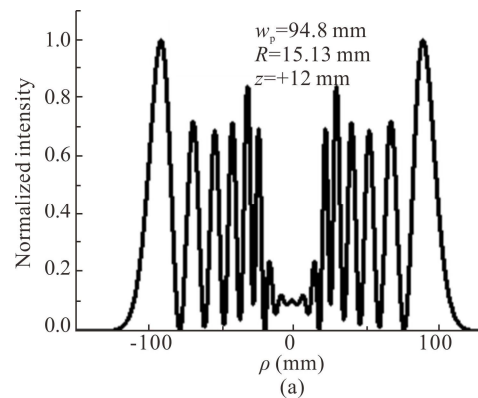
(b)
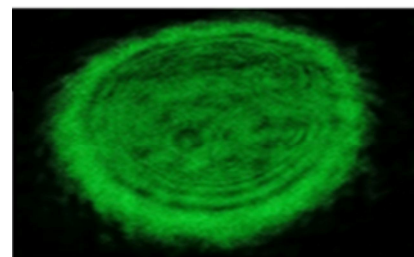
(c)

Fig.7 (a) Theoretical simulation result of the 2D intensity distribution at *z*=+12 mm by using Eq.(8); (b) 3D theoretical rings; (c) Experimental rings

w_p=229.4 mm
R=35.45 mm
z=+33 mm

(a)

(b)

(c)
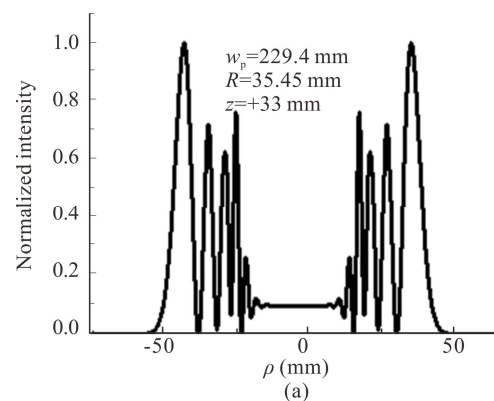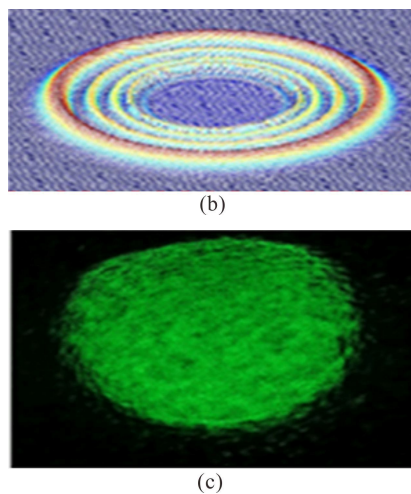
Fig.8 (a) Theoretical simulation result of the 2D intensity distribution at *z*=+33 mm by using Eq.(8); (b) 3D theoretical rings; (c) Experimental rings

This work presents an experimental far-field diffraction ring's pattern of laser beam after propagating through 8HQABS solution used as nonlinear medium. F-K diffraction integral was employed to obtain the simulated far-field diffraction ring patterns at three positions before focal plane. The numerical diffraction rings were compared with the experimental diffraction rings of 8HQABS solution, and they were in a good agreement.

Acknowledgements

Statements and Declarations

The authors declare that there are no conflicts of interest related to this article.

References

[1]   KARIMZADEH R. Spatial self-phase modulation of a laser beam propagating through liquids with self-induced natural convection flow[J]. Journal of optics, 2002, 14：095701.

[2]   MAJLES A M H, AKHERATDOOST H, KOUSHKI E. Self-diffraction and high nonlinear optical properties of carbon nanotubes under CW and pulsed laser illumination[J]. Journal of molecular liquids, 2015, 206：4 -9.

[3]   ELIAS R S, HASSAN Q M A, SULTAN H A, et al. Thermal nonlinearities for three curcuminoids measured by diffraction ring patterns and Z-scan under visible CW laser illumination[J]. Optics & laser technology, 2018, 107：131-141.

[4]   ZIDAN M D, Al-KTAIFANI M M, EL-DAHER M S, et al. Diffraction ring patterns and nonlinear measurements of the tris(2′,2-bipyridyl) iron(II) tetrafluoroborate[J]. Optics & laser technology, 2020, 131：106449.

[5]   CALLEN W R, HUTH B G, PANTELL R H. Optical patterns of thermally self-defocused light[J]. Applied physics letters, 1967, 11：103-105.

[6]   VILLAFRANCA A B, SARAYANAMUTTU K. Diffraction rings due to spatial self-phase modulation in a photopolymerizable medium[J]. Journal of optics A-pure and applied optics, 2009, 11：125202.

[7]   ZAMIR A Z, KARIMZADEH R, MANSOUR N. Thermo- optic properties and nonlinear responses of copper nanoparticles in polysiloxane oil[J]. Journal of optics, 2010, 12：035212.

[8]   PILLA V, MUNIN E, GESUALDI M R R. Measurement of the thermo-optic coefficient in liquids by laser-induced conical diffraction and thermal lens techniques[J]. Journal of optics A-pure and applied optics, 2009, 11：105201.

[9]   MAO Z, QIAO L, HE F, et al. Thermal-induced nonlinear optical characteristics of ethanol solution doped with silver nanoparticles[J]. Chinese optics letters, 2009, 7：949-952.

[10]   NEUPANE T, TABIBI B, SEO F J. Spatial self-phase modulation in WS_2 and MoS_2 atomic layers[J]. Optical materials express, 2020, 10：831-842.

[11]   ZHANG Q, CHENG X, ZHAN Y, et al. Optical limiting using spatial self-phase modulation in hot atomic sample[J]. Optics & laser technology, 2017, 88：54-60.

[12]   MAJLES A M H, SALMANI S, ESMAEILZADEH M, et al. Optical characterization of Erioglaucine using Z-scan technique, beam radius variations and diffraction pattern in far-field[J]. Current applied physics, 2009, 9：885-889.

[13]   KOUSHKI E, FARZANEH A, MOUSAVI S H. Closed aperture Z-scan technique using the Fresnel-Kirchhoff diffraction theory for materials with high nonlinear refractions[J]. Applied physics B, lasers and optics, 2010, 99：565-570.

[14]   ZIDAN M D, ARFAN A, EL-DAHER M S, et al. Synthesis and diffraction ring patterns of 8-hydroxy quinolin-1-ium4-amino-benzenesulfonate[J]. Optik, 2021, 223：167439.

[15]   ZIDAN M D, ALLAF A W, ALLAHHAM A, et al. Nonlinear optical study of chromium tetrapyrrole dicarbonyl [Cr(CO)2(Pyrrole)4] complex[J]. Optik, 2020, 200：163175.

[16]   GARCIA R E V, ARROYO C M L, MENDEZ O M M, et al. Far field intensity distributions due to spatial self-phase modulation of a Gaussian beam by a thin nonlocal nonlinear media[J]. Optics express, 2010, 18：22067-22079.

[17]   LIAO Y, SONG C, XIANG Y, et al. Recent advances in spatial self-phase modulation with 2D materials and its applications[J]. Annalen der physik, 2020, 532：2000322-2000350.

[18]   DENG L, HE K, ZHOU T, et al. Formation and evolution of far-field diffraction patterns of divergent and convergent Gaussian beams passing through self-focusing and self-defocusing media[J]. Journal of optics A-pure and applied optics, 2005, 7：409-415.